Experimental Observation of Discharge Characteristics Under Variable Ambient Temperature in AC Plasma Display Panel

Soo-Kwan Jang and Heung-Sik Tae, *Senior Member, IEEE*

***Abstract*—The effect of an ambient temperature ranging from -5 °C to $+65$ °C on the discharge characteristics was examined. The change in the firing voltage according to the ambient temperature was much higher under MgO cathode conditions with a high secondary electron emission coefficient than under phosphor cathode conditions with a low secondary electron emission coefficient. Through the weak reset discharge, the wall voltages were increased with an increase in the ambient temperature, as the wall charges were less erased at a higher ambient temperature during the ramp-down period. An increase in the ambient temperature was also found to have a more significant influence on the statistical delay time than on the formative delay time. Since the statistical delay time is strongly related to the priming condition, a higher ambient temperature may contribute to a better priming condition for reducing the statistical delay time during the address period.**

***Index Terms*—Address discharge, ambient temperature, discharge characteristics, V_t closed-curve.**

I. Introduction

ALTHOUGH the image quality of plasma display panels has continued to improve significantly [1], further advances in the image quality of ac-plasma display panels (ac-PDPs), particularly full high-definition PDPs, require a wider driving margin and more stable discharge. The ambient temperature is an important factor for producing the stable discharge in the PDP cells, as the discharge characteristics vary depending on the ambient temperature. However, research on the relation between the ambient temperature and the discharge characteristics has not been extensive [2], [3].

Accordingly, this paper examines the charges in the discharge characteristics, such as the reset, address, and sustain discharges, based on a variation in the firing voltage relative to a low or high ambient temperature ranging from -5 °C to $+65$ °C using the V_t closed-curve measurement method.

Manuscript received August 11, 2008; revised October 26, 2008. First published January 13, 2009; current version published February 11, 2009. This work was supported in part by the New Growth Engine project of the Ministry of Commerce, Industry, and Energy of Korea and in part by the Brain Korea 21 (BK21).

The authors are with the School of Electrical Engineering and Computer Science, Kyungpook National University, Daegu 702-701, Korea (e-mail: hstae@ee.knu.ac.kr; waterpipe@ee.knu.ac).

Color versions of one or more of the figures in this paper are available online at http://ieeexplore.ieee.org.

Digital Object Identifier 10.1109/TPS.2008.2009540

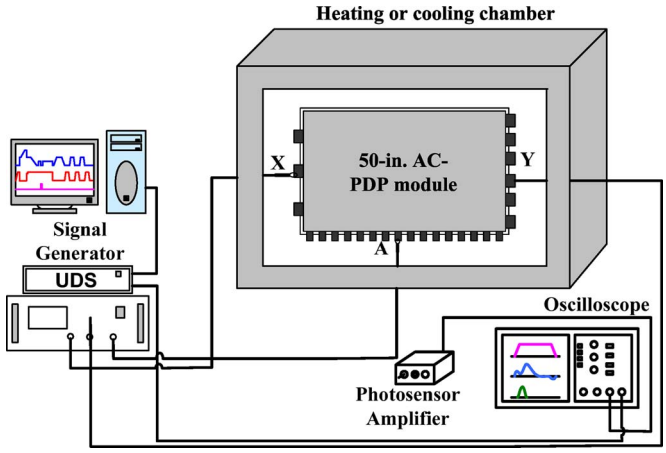

Fig. 1. Schematic diagram of experimental setup for the overall heating of the 50-in test panel with three electrodes, where X is common electrode, Y is scan electrode, and A is address electrode.

TABLE I
SPECIFICATIONS OF THE 50-in TEST PANEL EMPLOYED IN THE EXPERIMENTS

Specifications of 50-in. panel	
Pixel pitch	808 μm
Thickness of dielectric layer	30 μm
Rib Height	120 μm
Gas mixture	Ne – He(35%) – Xe (11 %),
Pressure	450 Torr
ITO width	310 μm
ITO gap	60 μm
Address electrode width	90 μm

II. Experimental Setup

Fig. 1 shows a schematic diagram of the experimental setup. A 50-in test panel with a working gas pressure of 450 torr was employed in this paper, and its structure and dimensions were the same as those of a conventional 50-in-wide eXtended Graphics Array-grade PDP with a box-type barrier rib. The gas mixtures used were He (35%)–Ne–Xe (11%), and the detailed panel specifications are listed in Table I. As shown in Fig. 1, the ambient temperature of the test panel was varied from -5 °C to $+65$ °C by heating or cooling the temperature test chamber. To avoid the influence of the ambient temperature on the

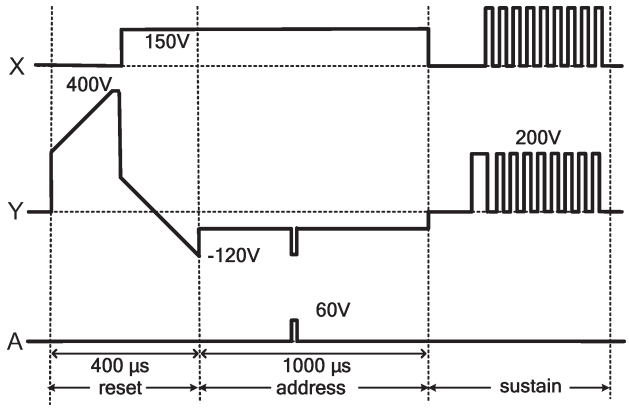

Fig. 2. Driving waveform employed for these experiments.

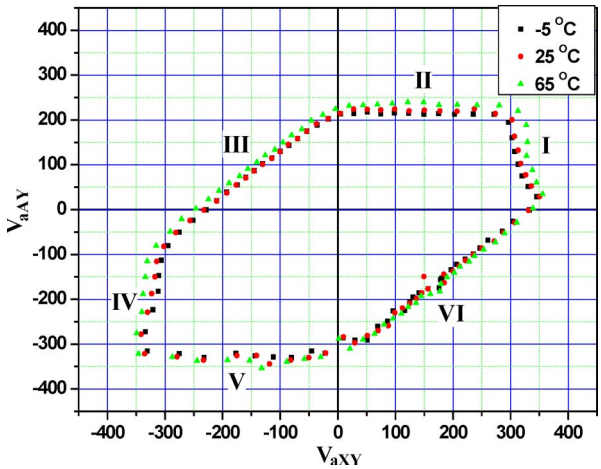

Fig. 3. V_t closed-curves measured from 50-in test panel under variable ambient temperatures, where Ⅰ, Ⅱ, Ⅲ, and Ⅳ are threshold voltages under MgO cathode discharge conditions and Ⅴ and Ⅵ are threshold voltages under phosphor cathode discharge conditions.

electronic circuit, all the electronics were positioned outside the temperature test chamber. Fig. 2 shows the driving waveform used to investigate the effect of the ambient temperature on the weak reset, the strong address, and the sustain discharge characteristics during the reset, address, and sustain periods, respectively.

III. Results and Discussion

A. Variation of Firing Voltages Relative to Ambient Temperatures

Fig. 3 shows the V_t closed-curves measured at three different ambient temperatures under zero initial wall voltage conditions. When the ambient temperature was increased from -5 °C to $+65$ °C, the area of the V_t closed-curve was increased, which means that the firing voltages among the three electrodes were increased under both phosphor and MgO cathode conditions. This phenomenon was mainly due to the fact that increasing the ambient temperature had the same effect as increasing the working gas pressure [4].

Fig. 4 shows the changes in the firing voltage relative to the ambient temperature under three different discharge conditions, where the Y–A discharge [Ⅴ] is the discharge produced between the Y–A electrodes under phosphor cathode conditions, while the X–Y [Ⅰ] and A–Y [Ⅱ] discharges are the discharges produced between the X–Y electrodes and between the A–Y electrodes, respectively, under MgO cathode conditions. As shown in Fig. 4, the ambient temperature had a more significant influence on changing the firing voltage under MgO cathode conditions than under the phosphor cathode condition. Under MgO cathode conditions with a higher secondary electron emission coefficient, increasing the ambient temperature from -5 °C to $+65$ °C caused an increase in the firing voltage of greater than 20 V, whereas under phosphor cathode conditions with a lower secondary electron emission coefficient, increasing the ambient temperature from -5 °C to $+65$ °C caused an increase in the firing voltage of less than 10 V. The change in the firing voltage according to the ambient temperature can be explained by the Paschen curve, which is described by the following [5]:

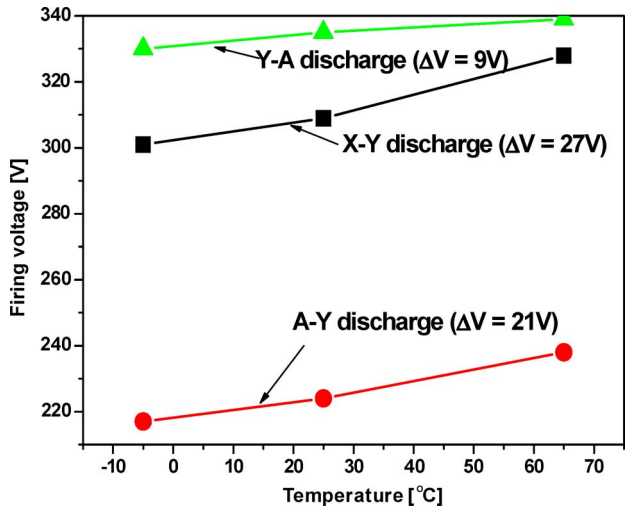

Fig. 4. Variation of firing voltage measured from a 50-in test panel under variable ambient temperatures; (Ⅰ) and (Ⅱ) are under MgO cathode discharge conditions, and (Ⅴ) is under phosphor cathode conditions.

$$V_b = \frac{Bpd}{C + \ln(pd)}$$
$$C = \ln\left(A / \ln\left(1 + \frac{1}{\gamma}\right)\right) \quad (1)$$

where V_b is the breakdown voltage, p is the gas pressure, d is the gap distance, A and B are the gas constants, and γ is the secondary electron emission coefficient for the cathode layer. If the other conditions remain constant, the Paschen curve expressing the change in the firing voltage will vary depending on the value of the secondary electron emission coefficient.

Fig. 5 shows the calculated Paschen curve relative to p (pressure) $\times$ d (gap distance) under various secondary electron emission coefficients (γ). In this experiment, for the surface gap, $p \cdot d = 450$ torr $\times$ 60×10^{-4} cm $= 2.7$ torr $\cdot$ cm, whereas for the plate gap, $p \cdot d = 450$ torr $\times$ 120×10^{-4} cm $=$ 5.4 torr $\cdot$ cm. Since increasing the ambient temperature means an increase in the pressure, the firing voltage is increased with an increase in the ambient temperature. However, the Paschen curve in Fig. 5 shows that the change in the firing voltage

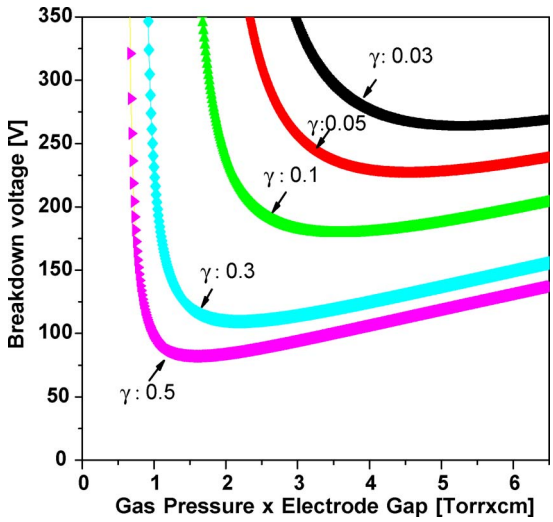

Fig. 5. Paschen curves showing the relation between the breakdown voltage and $p \cdot d$ under variable secondary electron emission coefficients (γ), where p is the gas pressure and d is the electrode gap.

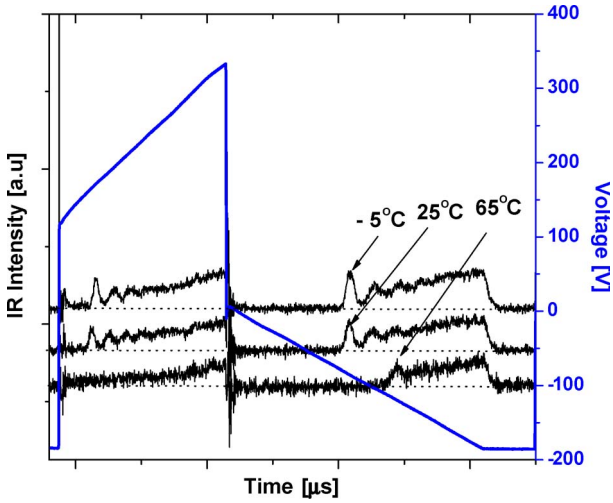

Fig. 6. IR (828 nm) intensities emitted during reset discharge measured from a 50-in test panel under variable ambient temperatures.

level according to the operating pressure strongly depended on the secondary electron emission coefficient (γ), i.e., a small secondary electron emission coefficient resulted in a small charge in the firing voltage with respect to $p \cdot d$. This means that the change in the firing voltage with the ambient temperature was much higher under MgO cathode conditions with a high secondary electron emission coefficient than under phosphor cathode conditions with a low secondary electron emission coefficient.

B. Characteristic of Reset Discharge Under Variable Ambient Temperatures

Fig. 6 shows the infrared (IR; 828 nm) intensities emitted during the reset discharge measured from a 50-in test panel under variable ambient temperatures. The variation in the firing voltage with the ambient temperature was large under MgO cathode conditions, yet small under phosphor cathode conditions. During the ramp-up period, the reset discharge was produced under both MgO and phosphor cathode conditions. The IR was emitted by the X–Y discharge under the MgO cathode condition during the forepart of the ramp-up period, whereas the IR was emitted by the Y–A discharge under the phosphor cathode condition during the latter part of the ramp-up period. Accordingly, at a higher ambient temperature of $+65$ °C, the IR was hardly emitted during the forepart of the ramp-up period; however, the IR was emitted during the latter part of the ramp-up period, as shown in Fig. 6. In contrast, during the ramp-down period, the reset discharge was only produced under MgO cathode conditions. Thus, during the ramp-down period, it was difficult to produce the erasing discharge at a higher ambient temperature due to the increase in the firing voltage with a higher ambient temperature. This means that the wall charges that accumulated on the three electrodes during the ramp-up period were less erased during the ramp-down period at a higher ambient temperature. Fig. 7(a)–(c) shows the shifts of the V_t closed-curves after the reset discharge with respect to the reference V_t closed-curve with a zero initial wall voltage at three different ambient temperatures. In Fig. 7, the voltage difference between the shifted and reference V_t closed-curves at each ambient temperature represents the final wall voltage induced by the wall charges formed during the ramp-up and ramp-down periods [6], [7]. Fig. 7(d) shows the wall voltages V_{wX-Y} and V_{wA-Y} obtained from the V_t closed-curve data in Fig. 7(a)–(c). As shown in Fig. 7(d), as the ambient temperature increased from -5 °C to $+65$ °C, the wall voltages V_{wX-Y} and V_{wA-Y} also increased, as the wall charges were less erased during the ramp-down period.

C. Characteristics of Address and Sustain Discharge Under Variable Ambient Temperatures

The address discharge is a strong discharge produced simultaneously between the A–Y and X–Y electrodes under MgO cathode conditions. Meanwhile, the sustain discharge is a strong discharge produced between the X–Y electrodes under the MgO cathode condition. The effects of the ambient temperature on these two strong discharges, i.e., the address and sustain discharges, are shown in Figs. 8–10.

Fig. 8 shows the changes in the IR (828 nm) intensities emitted during the address discharge at three different ambient temperatures: (a) -5 °C; (b) $+25$ °C; and (c) $+65$ °C. To measure the temporal dispersion of the address discharge, the IR emissions were measured repeatedly during the continuous 400 turn-address discharge so that the IR intensity profiles shown in Fig. 8 represent overlapped IR emission images. When the ambient temperature was increased from -5 °C to $+65$ °C, the IR emission intensity was decreased. In Fig. 8, the weakening of the IR emission intensity during the address discharge at $+65$ °C was mainly due to the increase in the firing voltage at $+65$ °C. In other words, increasing the ambient temperature from -5 °C to $+65$ °C caused an increase in the firing voltage between the A–Y electrodes by approximately 21 V, whereas increasing the ambient temperature from -5 °C to $+65$ °C caused an increase in the wall voltage between the A–Y electrodes approximately 13 V, as shown in Figs. 4 and 7 respectively. Consequently, the electric field between the

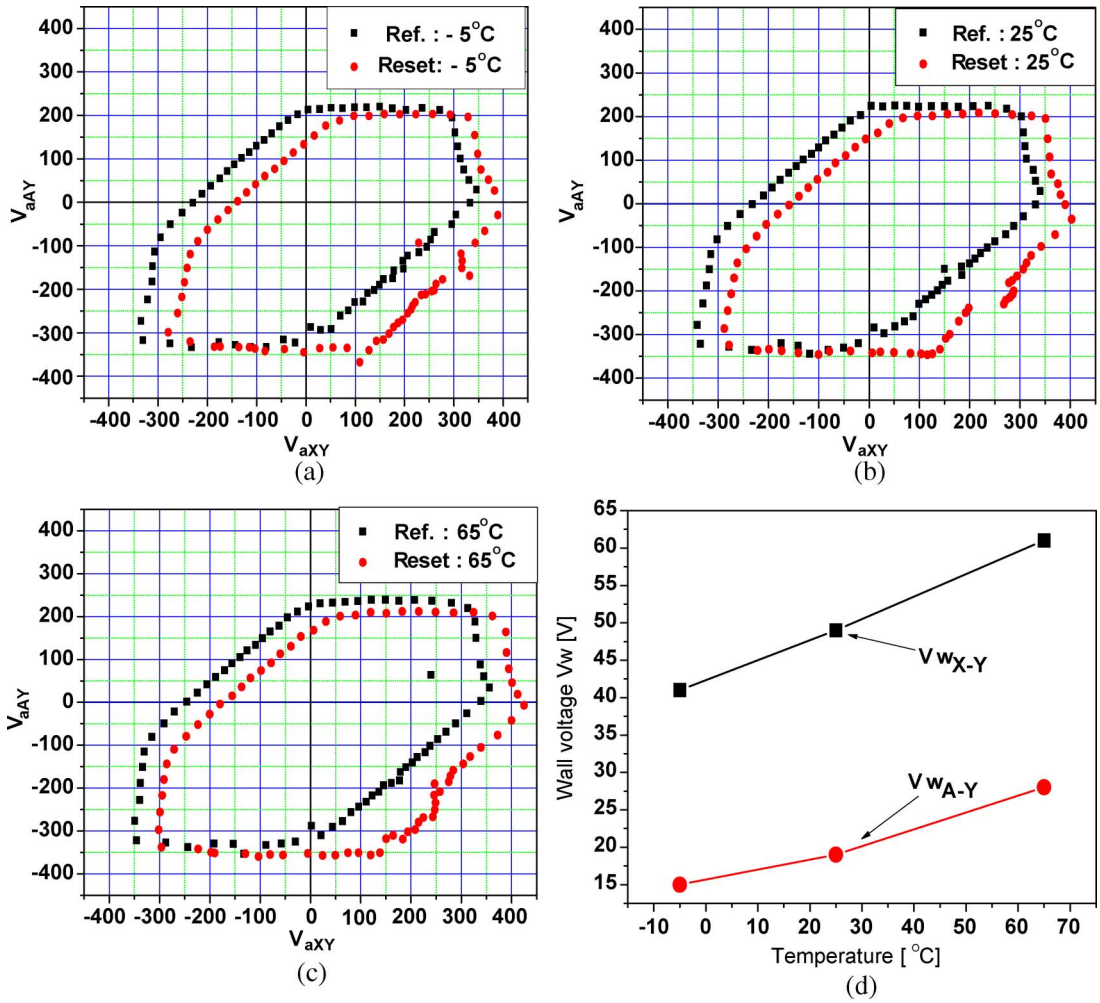

Fig. 7. Shifts of V_t closed-curves after reset discharge with respect to reference V_t closed-curve at three different ambient temperatures. (a) -5 °C. (b) $+25$ °C. (c) $+65$ °C. (d) Wall voltage, with V_{wX-Y} between the A–Y electrodes and the wall voltage and V_{wA-Y} between the X–Y electrodes induced by wall charges formed through a reset discharge relative to the ambient temperature.

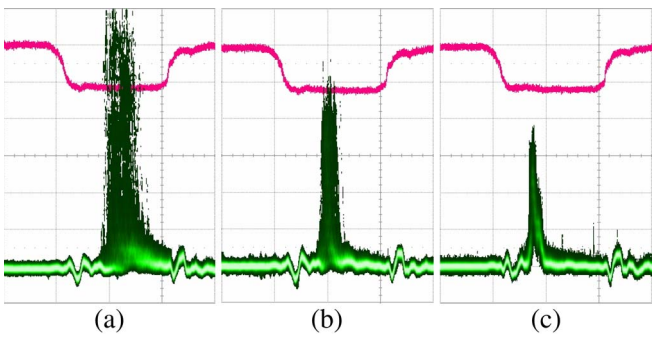

Fig. 8. IR (828 nm) intensities emitted during the address discharge at three different ambient temperatures (-5 °C, $+25$ °C, and $+65$ °C).

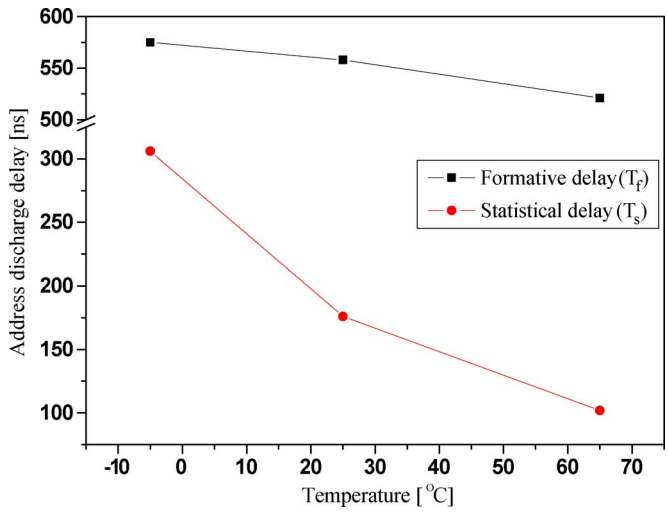

Fig. 9. Change in address discharge delays measured during address discharge from a 50-in test panel relative to ambient temperature.

A–Y electrodes was weaker at a higher ambient temperature. However, the dispersion of the IR emission was decreased irrespective of the weak IR emission intensity with an increase in the ambient temperature, as shown in Fig. 8. This phenomenon was related to the change of the priming condition according to the ambient temperature.

Fig. 9 shows the changes in the address discharge delay times relative to the ambient temperature. The address discharge delay time was measured 500 times under the same experimental conditions as in Fig. 8 [8]. At a higher ambient temperature, the formative delay (t_{f}) was decreased by approximately 74 ns, while the statistical delay time (t_{s}) was

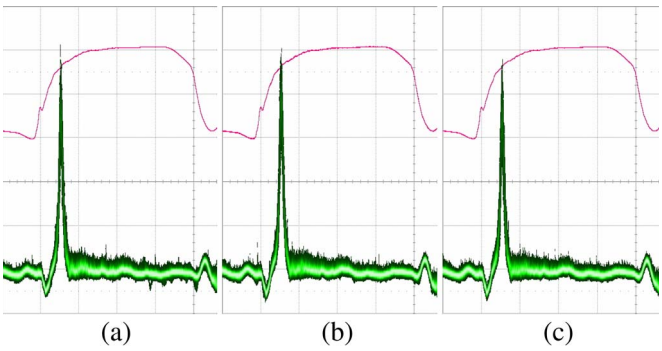

Fig. 10. IR (828 nm) intensities emitted during sustain discharge at three different ambient temperatures: (a) -5 °C. (b) $+25$ °C. (c) $+65$ °C.

decreased by approximately 204 ns. This means that increasing the ambient temperature had a much more significant influence on the statistical delay time than on the formative delay time. Since the statistical delay time is strongly related to the priming condition, the higher ambient temperature likely contributed to a better priming condition for reducing the statistical delay time. However, the better priming condition at a higher ambient temperature did not seem to have anything to do with the γ characteristics. If an increase in the γ value with the ambient temperature had caused the better priming condition, the firing voltage would not have increased with the ambient temperature. Therefore, this implies that the better priming condition with the ambient temperature is related to another phenomenon, such as the exoelectron emission phenomenon. However, this phenomenon needs to be studied further [9].

Fig. 10 shows the IR (828 nm) intensities emitted during the sustain discharge at three different ambient temperatures: (a) -5 °C; (b) $+25$ °C; and (c) $+65$ °C. To minimize the influence of the address discharge, the sustain discharge was measured during the tenth sustain discharge. As shown in Fig. 10, the IR emission intensity was slightly decreased at a higher ambient temperature, which means that the ambient temperature had little influence on the sustain discharge.

IV. Conclusion

The effect of an ambient temperature ranging from -5 °C to $+65$ °C on the firing voltage under MgO and phosphor cathode conditions was examined. The change in the firing voltage according to the ambient temperature was much higher under MgO cathode conditions with a high secondary electron emission coefficient than under phosphor cathode conditions with a low secondary electron emission coefficient. Through the weak reset discharge, the wall voltages were increased with the increase in the ambient temperature, as the wall charges were less erased at a higher ambient temperature during the ramp-down period. This was related to the increase in the firing voltage with the ambient temperature. It was also observed that the increase in the ambient temperature had a much more significant influence on the statistical delay time than the formative delay time. Since the statistical delay time is strongly related to the priming condition, a higher ambient temperature may contribute to a better priming condition for reducing the statistical delay time during the address period.

References

[1] L. F. Weber, "In celebration of 40 years of PDP history," in *Proc. IDW Dig.*, 2004, pp. 859–862.
[2] J.-H. Ryu, J.-Y. Choi, H.-J. Lee, D.-H. Kim, H. J. Lee, and C.-H. Park, "Experimental observation and modified driving method to improve the high-temperature misfiring in AC PDP," *IEEE Trans. Electron Devices*, vol. 51, no. 12, pp. 2026–2032, Dec. 2004.
[3] B. J. Shin, K. C. Choi, H.-S. Tae, J. H. Seo, J.-Y. Kim, and J.-W. Han, "Case studies on temperature-dependent characteristics in AC PDPs," *IEEE Trans. Plasma Sci.*, vol. 33, no. 1, pp. 162–169, Feb. 2005.
[4] S.-K. Jang, H.-S. Tae, E.-Y. Jung, K.-J. Suh, E.-G. Heo, and B.-H. Lee, "Modified ramp-reset waveform robust for ambient temperature in PDP," in *Proc. IDW Dig.*, 2006, pp. 1093–1096.
[5] W. S. Boyle and P. Kisliuk, "Departure from Paschen's law of breakdown in gases," *Phys. Rev.*, vol. 97, no. 2, pp. 255–259, Jan. 1955.
[6] K. Sakita, K. Takayama, K. Awamoto, and Y. Hashimoto, "High-speed address driving waveform analysis using wall voltage transfer function for three terminals and V_t close curve in three-electrode surface-discharge AC-PDPs," in *Proc. SID Dig.*, 2001, pp. 1022–1025.
[7] H.-S. Tae, S.-K. Jang, K.-D. Cho, and K.-H. Park, "High-speed driving method using bipolar scan waveform in AC plasma display panel," *IEEE Trans. Electron Devices*, vol. 53, no. 2, pp. 196–204, Feb. 2006.
[8] N. Uemura, Y. Yajima, M. Shibata, Y. Kawanami, and F. Namiki, "Improvement of the speed of address discharges in Ne–Xe–He discharge gases for ACPDPs," in *Proc. SID Dig.*, 2003, pp. 784–787.
[9] Q. F. Yan, N. Kosugi, Y. Oe, H. Tachibana, and L. F. Weber, "Analysis of priming source for addressing discharge of AC PDP," in *Proc. IDW Dig.*, 2006, pp. 359–362.

Soo-Kwan Jang received the B.S. and M.S. degrees in electronic and electrical engineering from Kyungpook National University, Daegu, Korea, in 2003 and 2006, respectively, where he is currently working toward the Ph.D. degree in electronic engineering in the School of Electrical Engineering and Computer Science.

His current research interests include plasma physics and driving waveforms of plasma display panels.

Heung-Sik Tae (M'00–SM'05) received the B.S., M.S., and Ph.D. degrees in electrical engineering from Seoul National University, Seoul, Korea, in 1986, 1988, and 1994, respectively.

Since 1995, he has been a Professor with the School of Electrical Engineering and Computer Science, Kyungpook National University, Daegu, Korea. His research interests include the optical characterization and driving waveforms of plasma display panels.

Dr. Tae is a member of the Society for Information Display. He has been serving as an Editor for the IEEE Transactions on Electron Devices section on display technology since 2005.